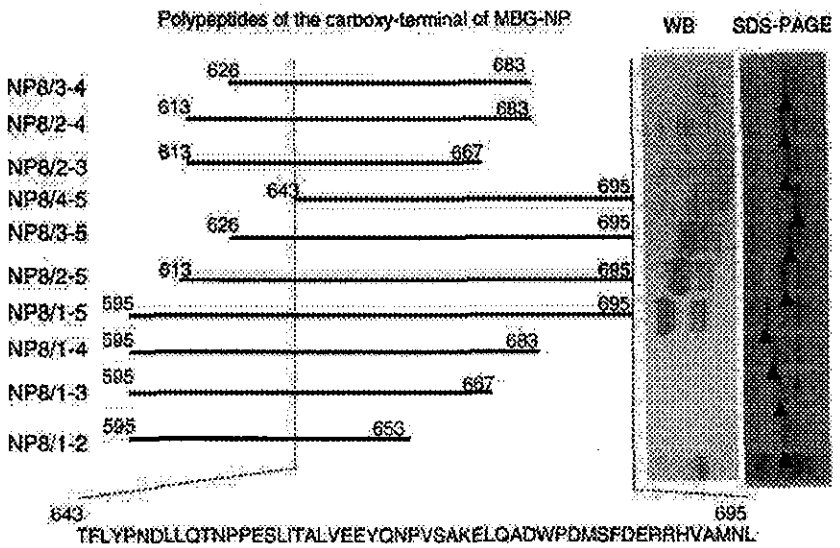

Fig. 4. Schematic representation of the truncated polypeptides (**left part**), expression levels of these polypeptides determined by SDS–PAGE analysis (right part, SDS–PAGE), and reactivity of MAb2H6 to these polypeptides in Western blotting (**right part**, WB). The numbers shown for each schematic polypeptide indicate the amino acid positions of the MBGV nucleoprotein.

(Fig. 6), indicating that the newly developed MBGV nucleoprotein-detection ELISA was specific for MBGV infections.

The amino acid sequence of the polypeptide recognized by MAb2A7 was conserved among Marburg virus isolates so far deposited in the GenBank, and there is no significant diversity in the amino acid sequences of the carboxy-terminal regions among Marburg virus isolates (http://www.ncbi.nlm.nih.gov/entrez/query.fcgi?db=Protein, Accession nos. AAR85460, AAR85453,

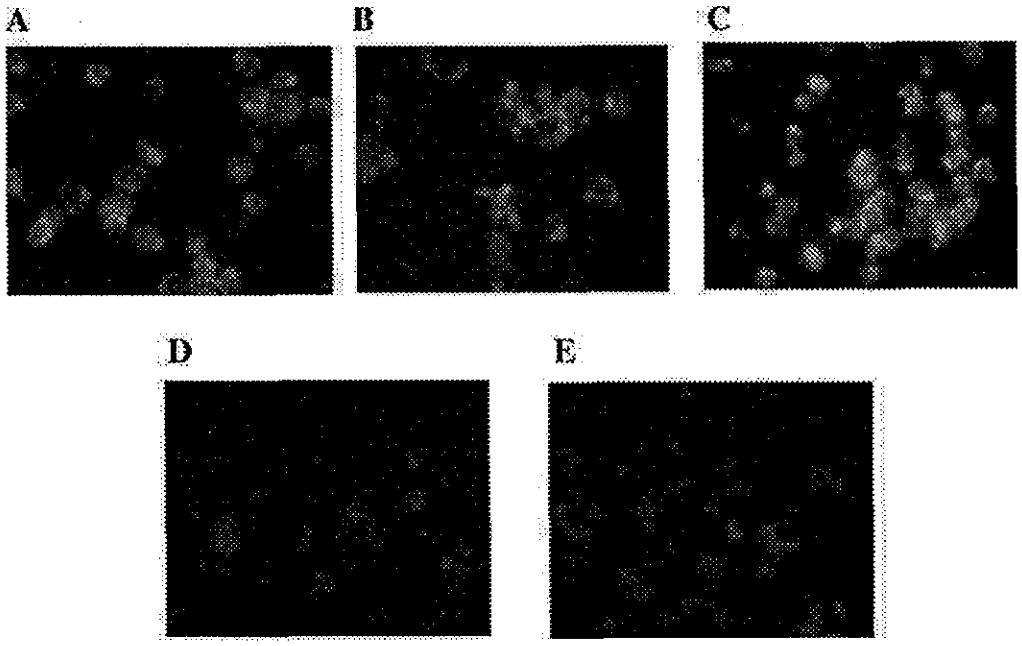

Fig. 5. Reactivity of MAb2A7 (**A**), MAb2H6 (**B**), anti-MBGV rNP rabbit serum (**C**), negative control mouse serum (**D**), and rabbit serum (**E**) to authentic MBGV antigens in Vero E6 cells in the immunofluorescence assay.

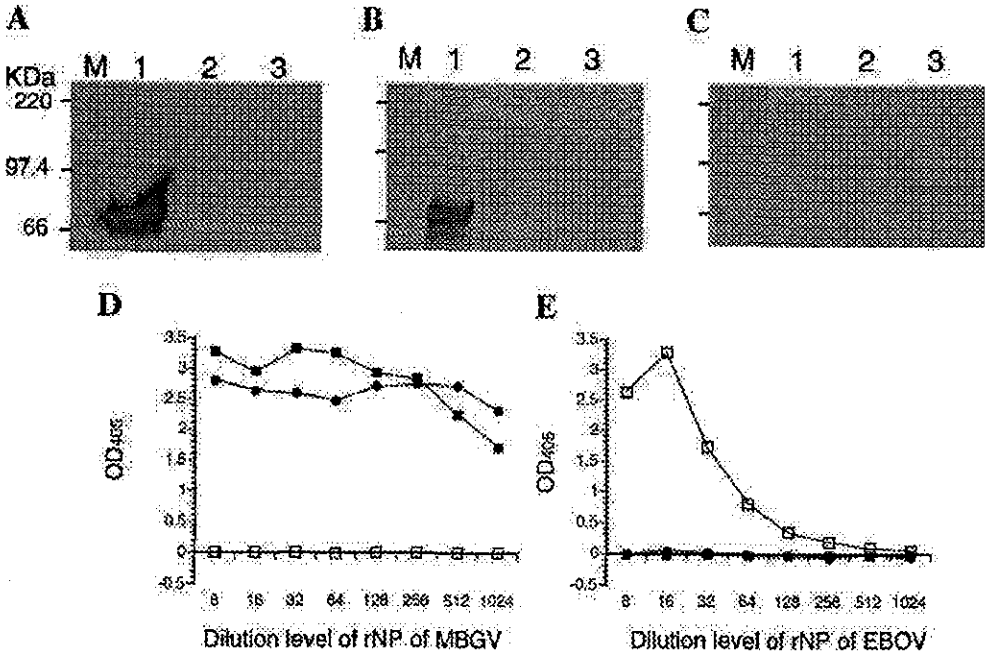

Fig. 6. Reactivity of the monoclonal antibodies to rNPs of MBGV and EBOV. Reactivity of MAb2A7 (**A**), MAb2H6 (**B**), and MAb3-3D (**C**) to MBGV rNP and EBOV rNP was examined in Western blotting. Lanes "M," "1," "2," and "3" indicate the lanes blotted with markers, GST-tagged MBG-NP/C-half, negative control antigen prepared from *Tn5* insect cells infected with the recombinant baculovirus without expression of foreign genes, and His-tagged rNP of EBOV, respectively [Saijo et al., 2001]. Reactivity of these monoclonal antibodies to the rNPs of MBGV (**D**) and EBOV (**E**) was also examined in the antigen-capture ELISA using MAb2A7 (■), MAb2H6 (●), or MAb3-3D (□).

NP_042025, AAQ55255, S44049, VHIWMV, P35263, 2110212A, P27588, CAA78114, CAA82536, AAA46563). Therefore, it is quite likely that the newly developed antigen-capture ELISA system for MBGV is useful for detecting most MBGV isolates, although further study is needed.

In conclusion, an MBGV nucleoprotein-detection ELISA system using unique monoclonal antibodies was developed, and the monoclonal antibodies useful for detecting nucleoprotein of the MBGV in the system were characterized. The combined use of the MBGV nucleoprotein-capture ELISA in the present study with the EBOV nucleoprotein-detection ELISA developed in a previous study [Niikura et al., 2001; Ikegami et al., 2003] may be useful for the diagnosis of viral hemorrhagic fevers due to filovirus infections.

ACKNOWLEDGMENTS

The study was performed with the approval of the ethical committee for animal experiments established in the National Institute of Infectious Diseases, Tokyo, Japan. We thank Prof. H.D. Klenk, Institute of Virology, Philipps-University, Marburg, Germany, for providing the DNA of the nucleoprotein of Marburg virus. We also thank Dr. J.B. McCormick, former head of the Special Pathogens Branch, Centers Disease Control and Prevention, Atlanta, GA, for providing the inactivated authentic Marburg virus antigens for IFA. We thank Ms. M. Ogata, Department of Virology 1, National Institute of Infectious Diseases, for her technical and clerical assistance.

REFERENCES

Anonymous. 1999. Marburg fever, Democratic Republic of the Congo. Wkly Epidemiol Rec 74:145.

Bausch DG, Borchert M, Grein T, Roth C, Swanepoel R, Libande ML, Talarmin A, Bertherat E, Muyembe-Tamfum JJ, Tugume B, Colebunders R, Konde KM, Pirad P, Olinda LL, Rodier GR, Campbell P, Tomori O, Ksiazek TG, Rollin PE. 2003. Risk factors for Marburg hemorrhagic fever, Democratic Republic of the Congo. Emerg Infect Dis 9:1531–1537.

Conrad JL, Isaacson M, Smith EB, Wulff H, Crees M, Geldenhuys P, Johnston JJ. 1987. Epidemiologic investigation of Marburg virus disease, Southern Africa, 1975. Am J Trop Med Hyg 27:1210–1215.

Drosten C, Gottig S, Schilling S, Asper M, Panning M, Schmitz H, Gunther S. 2002. Rapid detection and quantification of *RNA of* Ebola and Marburg viruses, Lassa virus, Crimean-Congo hemorrhagic fever virus, Rift Valley fever virus, dengue virus, and yellow fever virus by real-time reverse transcription-PCR. J Clin Microbiol 40:2323–2330.

Feldmann H, Slenczka W, Klenk HD. 1996. Emerging and reemerging of filoviruses. Arch Virol Suppl 11:77–100.

Gear JS, Cassel GA, Gear AJ, Trappler B, Clausen L, Meyers AM, Kew MC, Bothwell TH, Sher R, Miller GB, Schneider J, Koornhof HJ, Gomperts ED, Isaacson M, Gear JH. 1975. Outbreake of Marburg virus disease in Johannesburg. Br Med J 4:489–493.

Ikegami T, Niikura M, Saijo M, Miranda ME, Calaor AB, Hernandez M, Acosta LP, Manalo DL, Kurane I, Yoshikawa Y, Morikawa S. 2003. Antigen capture enzyme-linked immunosorbent assay for specific detection of Reston Ebola virus nucleoprotein. Clin Diagn Lab Immunol 10:552–557.

Johnson ED, Johnson BK, Silverstein D, Tukei P, Geisbert TW, Sanchez AN, Jahrling PB. 1996. Characterization of a new Marburg virus isolated from a 1987 fatal case in Kenya. Arch Virol Suppl 11:101–114.

Ksiazek TG, Rollin PE, Williams AJ, Bressler DS, Martin ML, Swanepoel R, Burt FJ, Leman PA, Khan AS, Rowe AK, Mukunu R, Sanchez A, CJ P. 1999. Clinical virology of Ebola hemorrhagic fever (EHF): Virus, virus antigen, and IgG and IgM antibody findings among EHF patients in Kikwit, Democratic Republic of the Congo, 1995. J Infect Dis 179:S177–S187.

Martini GA, Knauff HG, Schmidt HA, Mayer G, Baltzer G. 1968. [On the hitherto unknown, in monkeys originating infectious disease: Marburg virus disease]. Dtsch Med Wochenschr 93:559–571.

Niikura M, Ikegami T, Saijo M, Kurane I, Miranda ME, Morikawa S. 2001. Detection of Ebola viral antigen by enzyme-linked immunosorbent assay using a novel monoclonal antibody to nucleoprotein. J Clin Microbiol 39:3267–3271.

Peters CJ, LeDuc JW. 1999. An introduction to Ebola: The virus and the disease. J Infect Dis 179:ix–xvi.

Saijo M, Niikura M, Morikawa S, Ksiazek TG, Meyer RF, Peters CJ, Kurane I. 2001. Enzyme-linked immunosorbent assays for detection of antibodies to Ebola and Marburg viruses using recombinant nucleoproteins. J Clin Microbiol 39:1–7.

Sanchez A, Ksiazek TG, Rollin PE, Miranda ME, Trappier SG, Khan AS, Peters CJ, Nichol ST. 1999. Detection and molecular characterization of Ebola viruses causing disease in human and nonhuman primates. J Infect Dis 179:S164–S169.

Smith DH, Johnson BK, Isaacson M, Swanapoel R, Johnson KM, Killey M, Bagshawe A, Siongok T, Keruga WK. 1982. Marburg-virus disease in Kenya. Lancet 1:816–820.

JOURNAL OF CLINICAL MICROBIOLOGY, May 2004, p. 1869–1874 Vol. 42, No. 5
0095-1137/04/$08.00+0 DOI: 10.1128/JCM.42.5.1869–1874.2004

Specific Detection and Identification of Herpes B Virus by a PCR-Microplate Hybridization Assay

Chika Oya,[1,2] Yoshitsugu Ochiai,[1] Yojiro Taniuchi,[1]† Takashi Takano,[1]‡ Fukiko Ueda,[1] Yasuhiro Yoshikawa,[2] and Ryo Hondo[1]*

Department of Veterinary Public Health, Nippon Veterinary and Animal Science University, Musashino, Tokyo 180-8602,[1] and Department of Biomedical Science, Graduate School of Agricultural and Life Sciences, The University of Tokyo, Bunkyo-ku, Tokyo 113-8657,[2] Japan

Received 2 September 2003/Returned for modification 9 November 2003/Accepted 1 February 2004

Herpes B virus DNA was specifically amplified by PCR, targeting the regions that did not cross-react with herpes simplex virus (HSV). The amplified products, which were shown to be highly genetic polymorphisms among herpes B virus isolates, were identified by microplate hybridization with probes generated by PCR. The products immobilized in microplate wells were hybridized with the biotin-labeled probes derived from the SMHV strain of herpes B virus. The amplified products derived from the SMHV and E2490 strains of herpes B virus were identified by microplate hybridization. PCR products amplified from the trigeminal ganglia of seropositive cynomolgus macaques were identified as herpes B virus DNA. The utility of the PCR-microplate hybridization assay for genetic detection and identification of the polymorphic region of herpes B virus was determined.

Herpes B virus infection, caused by herpes B virus harbored in its natural host, Asian macaques, is a fatal encephalomyelitis in humans (6, 23, 26, 37). The primary means of transmission of herpes B virus to humans has been suggested to occur by direct and/or indirect contact with virus-contaminated secretion from the natural host (38). Forty-three cases of herpes B virus infection have been reported since the first reports by Sabin (7, 26). The infection has a high mortality if not treated by antiviral therapy in the early stages of infection. Thus, development of an assay is essential for prevention and early diagnosis of herpes B virus infection.

Herpes B virus is an alphaherpesvirus that shares some characteristics with the herpes simplex virus (HSV) (9). Both of the neurotropic viruses establish latency in the sensory nerve ganglia of their natural hosts (2, 34). Stress induces reactivation of the viruses from the latent state, resulting in shedding of infectious viruses from mucosal tissue (14, 35). In addition, herpes B virus shows strong serological cross-reactivity with HSV (5, 18). The genetic arrangement is almost identical between herpes B virus and HSV (8, 21, 22, 25), and the nucleotide sequences of the herpes B virus genes have been reported to show high homology with the corresponding HSV genes (1, 21, 22, 25). These similarities suggest that a sample from a patient with herpes B virus infection also contains HSV and that misidentification occurs in a diagnosis of the infection. In addition, HSV type 1 (HSV-1) was reported to be isolated and detected from a pet monkey and from white-faced monkeys with fatal infection, suggesting that a macaque, a natural host of herpes B virus, is infected with HSV (13, 30). Thus, accurate diagnosis of herpes B virus infection in both human and the natural herpes B virus host requires a specific assay to distinguish herpes B virus from the closely related HSV.

PCR was considered suitable for specific detection of herpes B virus. PCR was designed to amplify the herpes B virus target sequence, which is the most divergent in the genome sequence among HSV-1, HSV-2, and herpes B virus (4, 25). Furthermore, the amplified region was shown to have a highly genetic polymorphism among herpes B virus isolates derived from different natural host species (33). Thus, an applicable gene identification method is required to have the ability to identify the amplified products containing numerous point mutations. To overcome this difficulty, we developed a method of genetic identification by microplate hybridization with the probes generated by PCR.

MATERIALS AND METHODS

Virus. The inactivated herpes B virus E2490 strain isolated from a rhesus macaque was provided by Ryozaburo Mukai (National Institute of Infectious Diseases of Japan). The SMHV strain of herpes B virus was isolated from a cynomolgus macaque (1). Three isolates of HSV-1 (strains K8, K200, and 198) and three isolates of HSV-2 (strains 79-29, 27, and 111) were obtained from the vesicular fluid of patients with HSV reactivation. Four human cytomegalovirus (HCMV) isolates (strains Towne, AD169, KH, and OK-1) and two simian CMV (SCMV) isolates (strains 68-1 and 1090K) were used in the present study (36). HSV-1 and HSV-2 isolates were propagated in Vero cells, and HCMV and SCMV isolates were propagated in human embryonic lung cells.

Preparation of templates. A cloned 2.6-kb SalI-EcoRI fragment containing the US4, US5, and US6 genes from the SMHV strain (SMHV/pBV-DNA) was provided by Akio Yamada (National Institute of Infectious Diseases of Japan). Viral DNA from the E2490 strain was extracted and purified as previously described (11). Viral DNA from HSV-1, HSV-2, HCMV, and SCMV was extracted and purified from the infected cells according to a previously described procedure (11). Trigeminal ganglia from four healthy seropositive cynomolgus macaques were used as test samples. Both left and right ganglia were removed

* Corresponding author. Mailing address: Department of Veterinary Public Health, Nippon Veterinary and Animal Science University, 1-7-1 Kyonan, Musashino, Tokyo 180-8602, Japan. Phone: 81-422-31-4151, ext. 282. Fax: 81-422-30-7531. E-mail: nvau-vph@interlink.or.jp.

† Present address: Department of Molecular Immunology, Graduate School of Agricultural and Life Sciences, The University of Tokyo, Bunkyo-ku, Tokyo 113-8657, Japan.

‡ Present address: Laboratory Animal Research Center, The Institute of Medical Science, The University of Tokyo, Minato-ku, Tokyo 108-8639, Japan.

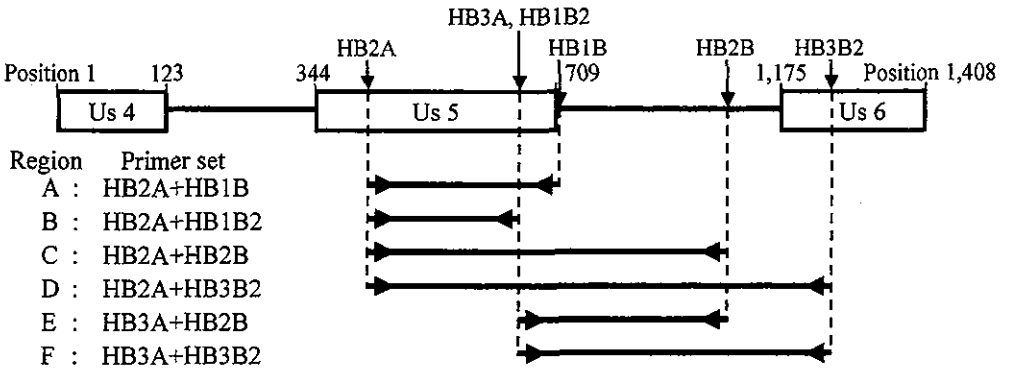

Primer	Sequence	Position
HB2A	5'-CCGCGCTCGCCACGGACACCA-3'	411-431
HB3A	5'-CCTGCACCGGTGCTGTAGACG-3'	643-663
HB1B	5'-TCGCGGGGTCACGCGTAGACG-3'	717-697
HB1B2	5'-CGTCTACAGCACCGGTGCAGG-3'	663-643
HB2B	5'-ATCGCGCGCCGGACCGATCGT-3'	1,072-1,052
HB3B2	5'-TCAGGGACCGCTCCACCGGCA-3'	1,274-1,254

FIG. 1. Target regions of PCR and primers used in the present study. Arrows on the genetic map indicate the locations of each primer. Open boxes indicate open reading frames of the 3′ side of the US4 gene, the complete US5 gene, and the 5′ side of the US6 gene. Nucleotide positions in this figure are cited as the E2490 strain sequence numbers deposited in the GenBank database (accession no. AF083210).

from the monkeys after rapid euthanasia following the intravenous injection of anesthesia. DNA was extracted and purified as described by Sambrook et al. (27). Purified DNA was stored at 4°C.

PCR. Design of the primers for herpes B virus DNA amplification referred to as nucleotide sequences US4 through US6 as determined by Bennett et al. (1) and Smith et al. (33). The GenBank accession numbers for the sequences cited in the present study are AF082804 to AF082814, AF083210, and S48101. A partial 330-bp gene encoding HSV DNA polymerase was amplified with the primer pair KM-1 (5′-CAGTACGGCCCCGAGTTCGTGACCGGG-3′) and KM-2 (5′-GGCGTAGTAGGGCGGGGATGTCGCG-3′) as described by Kimura et al. (17). The 610-bp fragments encoding part of HCMV and SCMV VP25 were amplified with the sense primer CM-3 (5′-ACTCACAACATATTC GTTTGC-3′) and the antisense primer CM-2 (5′-TGTTCGGAAGTGATCGT GTTT-3′) as described by Meigata et al. (19). PCR was performed in 100 μl of 1× *Ex Taq* Buffer (Takara Shuzo, Shiga, Japan), 0.2 mM (each) deoxynucleoside triphosphates, 0.5 μM concentrations of each of the primers, 0.5 U of *Ex Taq* polymerase (Takara Shuzo), and the template. The reaction was carried out for 30 cycles of denaturation at 94°C for 2 min, annealing at 55°C for 3 min, and extension at 72°C for 4 min. The amplified products were separated by electrophoresis on 1.5% agarose gels, stained with ethidium bromide, and visualized under a UV transilluminator.

Microplate hybridization. Microplate hybridization was performed as previously described (12, 15) with some modifications. Briefly, the heat-denatured PCR products were diluted by using 10-fold serial dilutions in coating buffer (1.5 M NaCl, 0.2 mM sodium phosphate [pH 7.4], 5 mM EDTA). The serially diluted products were allowed to adsorb to the microplate wells by incubation at 37°C for 3 h. Biotin-labeled probes were generated by PCR as described above, except for the use of Biotin 11-dUTP (Enzo Diagnostics, Inc.) in place of dTTP. Hybridization was performed at 42 and 56°C for 20 h. Hybridization signals were detected by binding streptavidin-conjugated β-galactosidase to biotinylated probes, followed by reaction with the 4-methylumbelliferyl-β-D-galactoside substrate. The amount of the fluorescent reactant was determined by measurement of the absorbance at 460 nm with a fluorometric microplate reader (Fluoroskan II; Labsystems, Tokyo, Japan) and calculated as fluorescence units (FU).

RESULTS

Design of primers of herpes B virus. Two sense primers (HB2A and HB3A) and four antisense primers (HB1B, HB1B2, HB2B, and HB3B2) were designed in the present study (Fig. 1). HB2B is located on a noncoding intergenic region between the US5 and US6 genes, whereas HB3B2 is located on part of the open reading frame of the US6 gene, and the remaining primers are located on part of the open reading frame of the US5 gene. Six regions, A to F (Fig. 1), were generated by gene amplification combining a sense primer and an antisense primer.

Specificity of PCR. PCR was performed with five different virus templates (SMHV/pBV-DNA, HSV-1, HSV-2, HCMV, and SCMV). Amplification of the A, C, and E regions successfully generated products from SMHV/pBV-DNA but not from HSV-1, HSV-2, HCMV, and SCMV isolates (Fig. 2). Amplified products of the A, C, and E regions were also detected from the E2490 strain of herpes B virus (Fig. 3). In contrast, amplification of the B and D regions yielded products from SMHV/pBV-DNA and the HSV-1 and HSV-2 isolates, which showed almost the same size bands on agarose gels (data not shown). A gene amplification targeting the F region also resulted in a product from the HSV-2 27 strain, although the fragment showed a different size band than that from the herpes B virus strain.

Sensitivity of PCR. Amplification of the A, C, and E regions was performed with DNA templates of serial 10-fold dilutions of SMHV/pBV-DNA from 10 ng to 10 fg. The bands of amplified products on agarose gels were confirmed under a UV transilluminator. PCR of the C region could generate the products from 10 fg of the plasmid DNA, whereas the detectable limits of PCR of the A and E regions were 1 pg and 100 fg of the templates, respectively (data not shown).

Microplate hybridization identification of the amplified herpes B virus product. The C region of the PCR product derived from SMHV/pBV-DNA was used as both DNA samples and

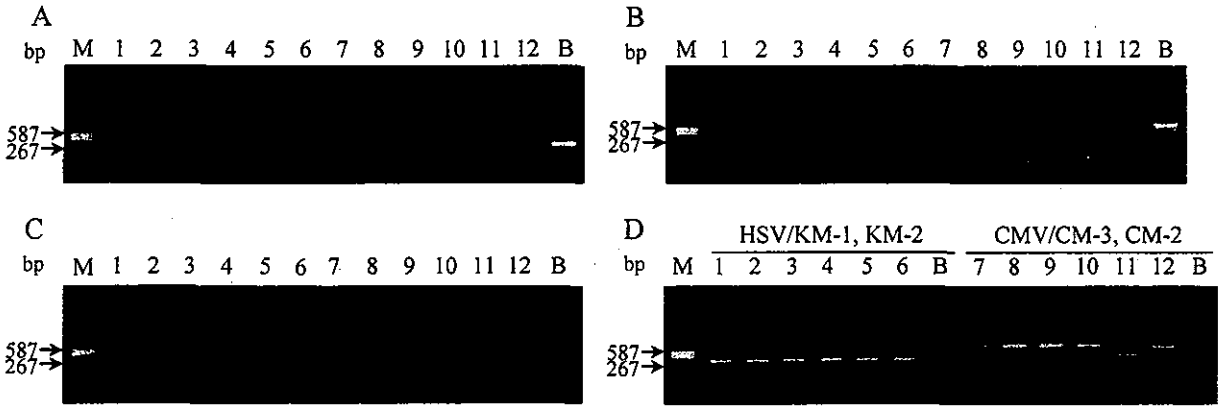

FIG. 2. Specific detection of herpes B virus by gene amplification of the A, C, and E regions (A, B, and C, respectively). (D) Amplification of HSV and CMV with each specific primer set (primer pairs KM1-KM2 and CM3-CM2, respectively). HSV-1 isolates are in lanes 1 to 3 (strains K8, K200, and 198, respectively); HSV-2 isolates are in lanes 4 to 6, (strains 79-29, 27, and 111, respectively); HCMV isolates are in lanes 7 to 10 (strains Towne, AD169, KH, and OK-1, respectively); and SCMV isolates are in lanes 11 and 12 (strains 68-1 and 1090K, respectively). Lanes B and M show SMHV/pBV-DNA and DNA standard size markers (DNA-Molecular Weight Marker V; Roche Diagnostics), respectively.

probes in this experiment. The products were diluted, and the resultant 10^{-2} to 10^{-6} dilutions were analyzed by microplate hybridization. Each diluted product was hybridized with the A- and C-region probes labeled with biotin and the resulting signal intensity was calculated as FU. The FU values were plotted against each dilution of the products. The resulting dilution curve was used to evaluate the identification of the amplified product. The hybridization curves, as shown in Fig. 4, were observed in conditions at both 42 and 56°C.

Genetic identification by microplate hybridization between heterogeneous amplified products. Heterogeneous hybridization was investigated by using the product amplified of the C region from the E2490 strain isolated from a rhesus macaque and the PCR product of the DNA polymerase gene derived from the HSV-1 HF strain. The products were hybridized with the C-region probe generated from SMHV/pBV-DNA. The nucleotide sequences of the C regions of the SMHV and the E2490 strains (GenBank accession no. S48101 and AF083210, respectively) share an 80.4% homology, while the product from HSV DNA polymerase shows no homology with the C region of the SMHV strain. Dilution curves obtained from hybridization of the E2490 and HSV HF strain are shown in Fig. 5. Specific hybridization signals were observed in dilution curves obtained from hybridization of the E2490 strain at both 42 and 56°C. In contrast, the FU values of the amplified products encoding the HSV HF strain DNA polymerase showed a curve almost identical to that of the negative control in hybridization at both 42 and 56°C.

Application to seropositive monkey specimens. PCR-microplate hybridization was applied to the trigeminal ganglia of four seropositive cynomolgus monkeys. Amplified products of the C region were detected in all seropositive macaque specimens. The products generated from two seropositive specimens showed a smaller band size than the corresponding C

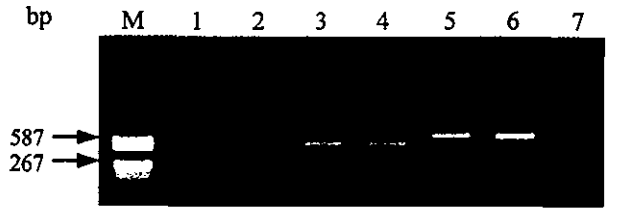

FIG. 3. Agarose gel electrophoresis of the amplified products derived from the herpes B virus strains. The gene amplification was performed to yield the C-region products with the primer pair HB2A-HB2B. The amplified products derived from the seropositive monkey specimens are in lanes 1 to 4, the E2490 strain is in lane 5, and SMHV/pBV-DNA is in lane 6. The PCR reactant of the negative control is in lane 7. A difference in band size can be seen between the PCR products generated from the E2490 strain or SMHV/pBV-DNA and that from the seropositive monkeys (specimens 3 and 4 for lanes 3 and 4, respectively).

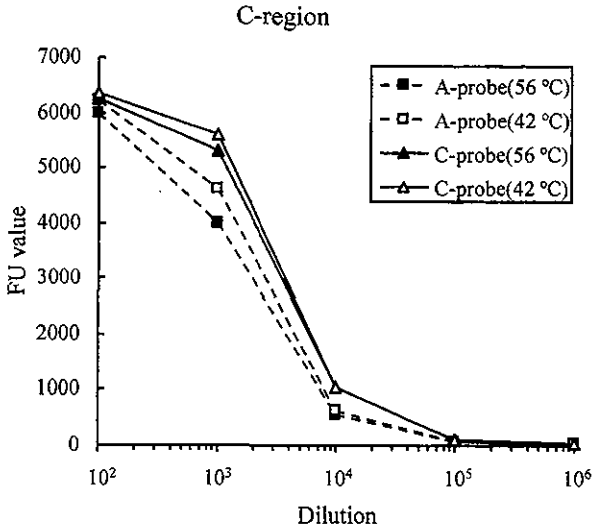

FIG. 4. Dilution curves from serial dilutions of the amplified product of the C regions. FU values were obtained by hybridization with probes from the A (squares) and C (triangles) regions at 56°C (solid symbols) and 42°C (open symbols). Dilution curves obtained by using the probes from the A and C regions are shown by dotted and solid lines, respectively.

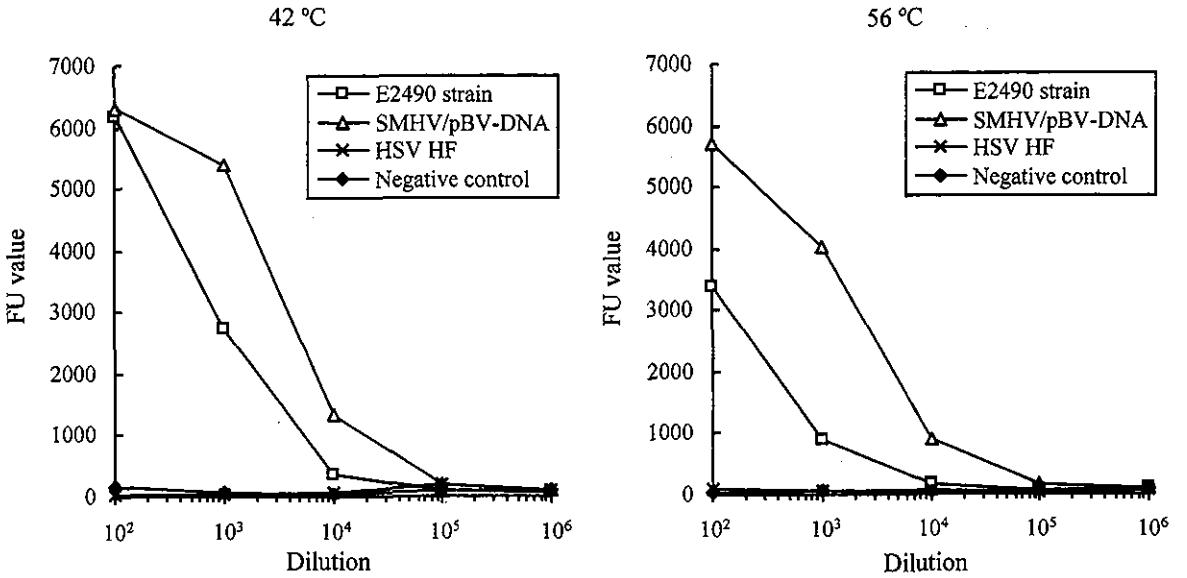

FIG. 5. Dilution curves of herpes B virus amplified products (E2490 strain and SMHV/pBV-DNA) and the HSV-1 HF strain obtained by PCR-microplate hybridization. Microplate hybridization with probes from the C regions was performed at 56°C (right) and 42°C (left). FU values are shown for E2490 (□), SMHV/pBV-DNA (△), HSV HF (×), and negative control (◆).

regions of the SMHV and E2490 strains, whereas DNA bands from the other specimens showed the same size as those from the known herpes B virus strains (Fig. 3). Serial dilutions of the product were hybridized with the probe of the C region at 42 and 56°C. The specific hybridization signals were obtained from the serial dilutions of the PCR products from the two seropositive specimens, which were the same size as the SMHV and E2490 products, by hybridization at both 42 and 56°C (Fig. 6, specimens 1 and 2). In the experiment with products that had sizes different from those of the known herpes B virus strains, the FU values obtained from hybridization at 56°C were almost identical to those of the negative control over the entire range of dilutions, whereas the specific signals were obtained from hybridization at 42°C (specimens 3 and 4).

DISCUSSION

Virus isolation in cell lines has been the standard method for diagnosis of a herpes B virus infection, even though contact with herpes B virus-contaminated specimens is extremely haz-

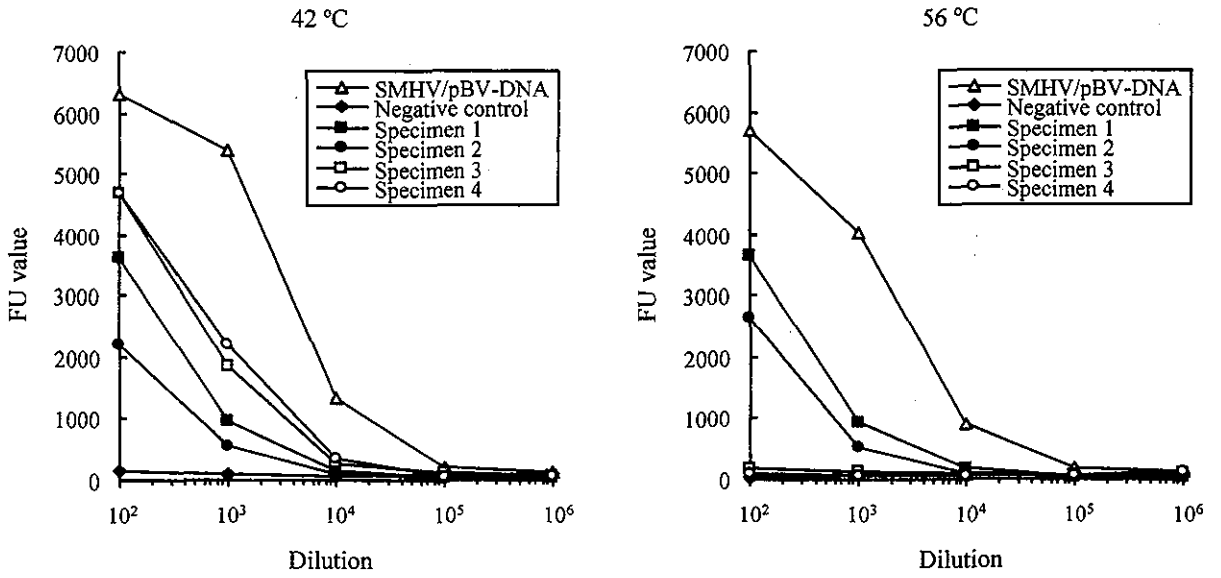

FIG. 6. Dilution curves of herpes B virus amplified products of seropositive monkey specimens (specimens 1 to 4) and SMHV/pBV-DNA obtained by PCR-microplate hybridization. Microplate hybridization with probes from the C regions was performed at 56°C (right) and 42°C (left). FU values are shown for seropositive specimens (■, ●, □, and ○ for specimens 1 to 4, respectively), SMHV/pBV-DNA (△), and a negative control (◆).

ardous and requires a level 3 or higher biosafety containment facility (3). In order to avoid the danger of working with virus-contaminated specimens, sensitive and less-hazardous PCR methods of detection have been developed (31, 32). A specific herpes B virus detection method is also necessary in order to distinguish herpes B virus from the closely related HSV. In the present study, we designed PCR to amplify the regions of the US5 gene encoding glycoprotein J, which was shown to be the most divergent of the protein-coding genes in HSV-1, HSV-2, and herpes B viruses (4, 25) and the 3′-flanking noncoding intergenic region.

Herpesviruses have been reported to show intraspecies gene diversity among clinical isolates (20, 28, 29, 36). Thus, to investigate the specificity of the gene amplification, PCR was performed on templates from the HSV-1, HSV-2, HCMV, and SCMV isolates, which were confirmed to show a distinct genetic pattern in each herpesvirus. In gene amplification of the A, C, and E regions, no PCR products were detected from the isolates of the four species of herpesviruses. All amplified products, however, were detected from the herpes B virus E2490 and SMHV strains. PCR with the templates of serial 10-fold dilutions indicated that the gene amplification of the C region had the highest sensitivity in the products of the specific A, C, and E regions. The specificity and sensitivity of PCR suggest that amplification of the C region with the primer pair HB2A and HB2B is most suitable for the genetic detection of herpes B virus.

Microplate hybridization was performed with the A- or C-region probes generated by PCR, as reported previously on the development and application for diagnosis of varicella-zoster virus infection (10, 12, 15). Real-time PCR, however, a rapid genetic detection and identification method with oligonucleotide probes, has been developed for the diagnosis of herpes B virus infection (14, 24). The amplified region targeted in the present study showed a high degree of polymorphism among herpes B virus isolates (33), suggesting the presence of numerous point mutations. Thus, oligonucleotide probes were not likely to be available for the identification of variable amplified products because a point mutation has a great effect on the hybridization ability of an oligonucleotide probe, thus causing problems when we have limited gene information. In the present study, the full-length probe generated from the SMHV strain hybridized with PCR products derived not only from the SMHV strain but also from E2490 and seropositive specimen-derived strains, suggesting that the probe is useful for genetic identification of the herpes B virus.

The PCR product generated from the E2490 strain was observed to hybridize with the probe of the SMHV strain under high- and low-stringency conditions. On the other hand, the amplified products from two of four seropositive specimens were hybridized with the SMHV strain probe only under the low-stringency conditions, a finding consistent with the previous results of microplate hybridization between HSV-1 and HSV-2 (16). These results suggest that the genetic distance between the PCR products of the SMHV strain and seropositive specimen-derived strains is greater than the distance between those of the E2490 and SMHV strains. The results of gel electrophoresis, in which the DNA bands of the seropositive specimens showed a size distinct from those of the SMHV or E2490 strains, support this suggestion. Thus, the results indicate the possibility of failure to identify the herpes B virus product by hybridization under the high-stringency conditions if the nucleotide sequence identity between the PCR product and the probe is <80%, the identity level of the C region between the SMHV and E2490 strain. In conclusion, hybridization under low-stringency conditions may be indispensable for correct identification of the PCR product.

In summary, we developed a PCR-microplate hybridization assay for the detection and identification of PCR products derived from herpes B virus; this assay is able to detect herpes B virus but not HSV. The assay will be helpful in diagnosing humans suspected to have been exposed to herpes B virus, even if they are infected with HSV. In addition, the assay is a powerful tool for detecting and identifying unknown or new herpes B virus genotypes in both natural and human hosts. The relationship between the FU values and the serial dilutions of the PCR products suggests that the PCR-microplate hybridization assay technique may be useful in quantifying the herpes B virus genome.

ACKNOWLEDGMENTS

We thank to Ryozaburo Mukai and Akio Yamada for providing viral strains and recombinant plasmids, respectively.

This study was supported by a grant-in-aid for the Emerging and Re-emerging Disease project from the Ministry of Health, Labor, and Welfare of Japan.

REFERENCES

1. **Bennett, A. M., L. Harrington, and D. C. Kelly.** 1992. Nucleotide sequence analysis of genes encoding glycoproteins D and J in simian herpes B virus. J. Gen. Virol. 73:2963–2967.
2. **Boulter, E. A.** 1975. The isolation of monkey B virus (*Herpesvirus simiae*) from the trigeminal ganglia of a healthy seropositive rhesus monkey. J. Biol. Stand. 3:279–280.
3. **Cohen, J. I., D. S. Davenport, J. A. Stewart, S. Deitchman, J. K. Hilliard, L. E. Chapman, et al.** 2002. Recommendations for prevention of and therapy for exposure to B virus (*Cercopithecine Herpesvirus 1*). Clin. Infect. Dis. 35: 1191–1203.
4. **Doran, A., F. E. Jamieson, C. Cunningham, B. C. Barnett, and D. J. McGeoch.** 1998. The genome sequence of herpes simplex virus type 2. J. Virol. 72:2010–2021.
5. **Eberle, R., D. Black, and J. K. Hilliard.** 1989. Relatedness of glycoproteins expressed on the surface of simian herpes-virus virions and infected cells to specific HSV glycoproteins. Arch. Virol. 109:233–252.
6. **Eberle, R., and J. Hilliard.** 1995. The simian herpesviruses. Infect. Agents Dis. 4:55–70.
7. **Engel, G. A., L. Jones-Engel, M. A. Schillaci, K. G. Suaryana, A. Putra, A. Fuetes, and R. Henkel.** 2002. Human exposure to herpesvirus B-seropositive *macaques*, Bali, Indonesia. Emerg. Infect. Dis. 8:789–795.
8. **Harrington, L., Wall, L. V. M., and D. C. Kelly.** 1992. Molecular cloning and physical mapping of the genome of simian herpes B virus and comparison of genome organization with that of herpes simplex virus type 1. J. Gen. Virol. 73:1217–1226.
9. **Hilliard, J. K., D. Black, and R. Eberle.** 1987. Simian alphaherpesviruses and their relation to the human herpes simplex viruses. Arch. Virol. 109:83–102.
10. **Hiroshige, K., M. Ikeda, and R. Hondo.** 2002. Detection of varicella-zoster virus DNA in tear fluid and saliva of patients with Ramsay Hunt syndrome. Otol. Neurotol. 23:602–607.
11. **Hondo, R., Y. Yogo, T. Kurata, and Y. Aoyama.** 1987. Genome variation among varicella-zoster virus isolates derived from different individuals and from the same individuals. Arch. Virol. 93:1–12.
12. **Hondo, R., S. Ito, and S. Inoue.** 1995. Titration of varicella-zoster virus DNA in throat swabs from varicella patients by combined use of PCR and microplate hybridization. Jpn. J. Med. Sci. Biol. 48:249–255.
13. **Huemer, H. P., C. Larcher, T. Czedik-Eysenberg, N. Nowotny, and M. Reifinger.** 2002. Fatal infection of a pet monkey with human herpesvirus 1. Emerg. Infect. Dis. 8:639–641.
14. **Huff, J. L., R. Eberle, J. Capitanio, S. S. Zhou, and P. A. Barry.** 2003. Differential detection of B virus and rhesus cytomegalovirus in rhesus macaques. J. Gen. Virol. 84:83–92.
15. **Inoue, S., and R. Hondo.** 1990. Microplate hybridization of amplified viral DNA segment. J. Clin. Microbiol. 28:1469–1472.
16. **Inoue, S., and R. Hondo.** 1993. Type differentiation of herpes simplex virus

by stringent hybridization of polymerase chain reaction products. Arch. Virol. 129:311–316.
17. **Kimura, H., M. Futamura, H. Kito, T. Ando, M. Goto, K. Kuzushima, M. Shibata, and T. Morishima.** 1991. Detection of viral DNA in neonatal herpes simplex virus infections: frequent and prolonged presence in serum and cerebrospinal fluid. J. Infect. Dis. 164:289–293.
18. **Lees, D. N., A. Baskeville, L. M. Cropper, and D. W. Brown.** 1991. Herpesvirus simiae (B virus) antibody response and virus shedding in experimental primary infection of cynomolgus monkeys. Lab. Anim. Sci. 41:360–364.
19. **Meigata, K., R. Hondo, A. Fujiyama, M. Shinkai-Shibata, S. Itoh, Y. K. Kikuchi, Ando, N. Ichikawa, Y. Nomura, K. Watanabe, Y. H. Degawa, Beck, S. Tomikawa, T. Nagao, and H. Uchida.** 1996. Titration of human cytomegalovirus (HCMV) DNA in urine by combined use of PCR and microplate hybridization in a renal transplant patient with HCMV pneumonitis. Jpn. J. Med. Sci. Biol. 49:121–127.
20. **Meyer-Konig, U., M. Haberland, von Laer, D., O. Haller, and F. T. Hufert.** 1998. Intragenic variability of human cytomegalovirus glycoprotein B in clinical strains. J. Infect. Dis. 177:1162–1169.
21. **Ohsawa, K., D. H. Black, H. Sato, and R. Eberle.** 2002. Sequence and genetic arrangement of the US region of the monkey B virus (*Cercopithecine Herpesvirus* 1) genome and primate herpesviruses. J. Virol. 76:1516–1520.
22. **Ohsawa, K., D. H. Black, H. Sato, K. Rogers, and R. Eberle.** 2003. Sequence and genetic arrangement of the UL region of the monkey B virus (*Cercopithecine Herpesvirus* 1) genome and comparison with the UL region of other primate herpesviruses. Arch. Virol. 148:989–997.
23. **Palmer, A. E.** 1987. B virus, *Herpesvirus simiae*: historical perspective. J. Med. Primatol. 16:99–130.
24. **Perelygina, L., I. Patrusheva, N. Manes, M. J. Wildes, P. Krug, and J. K. Hilliard.** 2003. Quantitative real-time PCR for detection of monkey B virus (*Cercopithecine Herpesvirus 1*) in clinical samples. J. Virol. Methods 109:245–251.
25. **Perelygina, L., L. Zhu, H. Zurkuhlen, R. Mills, M. Borodovsky, and J. K. Hilliard.** 2003. Complete sequence and comparative analysis of the genome of herpes B virus (*Cercopithecine Herpesvirus 1*) from a rhesus monkey. J. Virol. 77:6167–6177.
26. **Sabin, A. B., and W. M. Wright.** 1934. Acute ascending myelitis following a monkey bite, with isolation of a virus capable of reproducing the disease. J. Exp. Med. 59:115–136.
27. **Sambrook, J., E. F. Fritsch, and T. Maniatis.** 1989. Molecular cloning: a laboratory manual, 2nd ed. Cold Spring Harbor Laboratory, Cold Spring Harbor, N.Y.
28. **Sakaoka, H., T. Aomori, O. Honda, Y. Saheki, S. Ishida, S. Yamanishi, and K. Fujinaga.** 1985. Subtypes of herpes simplex virus type1 in Japan: classification by restriction endonucleases and analysis of distribution. J. Infect. Dis. 152:190–197.
29. **Sakaoka, H., T. Kawana, L. Grillner, T. Aomori, T. Yamaguchi, H. Saito, and K. Fuginaga.** 1987. Genome variations in herpes simplex virus type2 strains isolated in Japan and Sweden. J. Gen. Virol. 68:2105–2116.
30. **Schrenzel, M. D., G. K. Osborn, A. Shima, R. B. Klieforth, and G. A. Maalfouf.** 2003. Naturally occurring fatal herpes simplex virus 1 infection in a family of white-faced saki monkeys (*Pithecia pithecia pithecia*). J. Med. Primatol. 32:7–14.
31. **Scinicariello, F., R. Eberle, and J. K. Hilliard.** 1993. Rapid detection of B virus (*Herpesvirus simiae*) DNA by polymerase chain reaction. J. Infect. Dis. 168:747–750.
32. **Slomka, M. J., D. W. Brown, J. P. Clewley, A. M. Bennett, L. Harrington, and D. C. Kelley.** 1993. Polymerase chain reaction for detection of *Herpesvirus simiae* (B virus) in clinical specimens. Arch. Virol. 131:89–99.
33. **Smith, A. L., D. H. Black, and R. Eberle.** 1998. Molecular evidence for distinct genotypes of monkey B virus (*Herpesvirus simiae*) which are related to the macaque host species. J. Virol. 72:9224–9232.
34. **Vizoso, A. D.** 1975. Recovery of *Herpes simiae* (B virus) from both primary and latent infections in rhesus monkeys. Br. J. Exp. Pathol. 56:485–488.
35. **Wagner, E. K., and D. C. Bloom.** 1997. Experimental investigation of herpes simplex virus latency. Clin. Microbiol. Rev. 10:419–443.
36. **Watanabe, S., M. Shinkai, S. Hitomi, H. Kozuka, S. Kimura, K. Shimada, R. Hondo, and N. Yamaguchi.** 1994. A polymorphic region of the human cytomegalovirus genome encoding putative glycoproteins. Arch. Virol. 137:11–121.
37. **Weigler, B. J.** 1992. Biology of B virus in macaque and human hosts: a review. Clin. Infect. Dis. 14:555–567.
38. **Weigler, B. J., D. W. Hird, J. K. Hilliard, N. W. Lerche, J. A. Robert, and L. M. Scott.** 1993. Epidemiology of *Cercopithecine Herpesvirus 1* (B virus) infection and shedding in a large breeding cohort of rhesus macaques. J. Infect. Dis. 167:257–263.

Arch Virol (2004) 149: 1279–1292
DOI 10.1007/s00705-004-0306-y

Archives of Virology
Printed in Austria

Modification of endothelial cell functions by hantaan virus infection: prolonged hyper-permeability induced by TNF-alpha of hantaan virus-infected endothelial cell monolayers

M. Niikura[1], A. Maeda[1], T. Ikegami[1,2], M. Saijo[1], I. Kurane[1], and S. Morikawa[1]

[1]Department of Virology 1, National Institute of Infectious Diseases, Musashimurayama, Japan
[2]Department of Biomedical Science, Graduate School of Agricultural and Life Sciences, The University of Tokyo, Tokyo, Japan

Received November 26, 2003; accepted January 28, 2004
Published online March 25, 2004

Summary. Serious vascular leakage is central to the pathogenesis of hantavirus infections. However, there is no evidence suggesting the hantavirus infection of endothelial cells directly causes obvious cell damage or morphological alteration either *in vivo* or *in vitro*. In this study, we examined whether Hantaan virus (HTNV) infection modifies the barrier function of endothelial cell monolayers upon the exposure to pro-inflammatory cytokines. Low levels (1 ng/ml) of tumor necrosis factor-alpha initially increased the permeability in both HTNV-infected and uninfected monolayers similarly. Thereafter, however, these monolayers showed significant difference. The HTNV-infected monolayers remained irreversibly hyper-permeable during the experimental period up to 4 days, while the uninfected monolayers completely recovered the barrier function. The prolonged hyper-permeability of HTNV-infected monolayers was not associated with cell death or gap formation in the monolayers, and was independent from their nitric oxide or prostaglandin production. These results are the first evidence that hantavirus infection modifies barrier function of endothelial cell monolayers and suggest that HTNV-infection of endothelial cells may contribute to the increased vascular leakage through the prolonged response to cytokines.

Introduction

Hantaviruses belong to the family *Bunyaviridae* and are transmitted to humans from various species of rodents, which are the natural reservoirs. Hantaviruses

consist of numerous strains and each strain is maintained in different rodent species in a natural environment [31]. It is believed that the geographical isolation of these host species contributes to the regional variation in the virulence of hantaviruses [38]. The severest forms of the hantavirus infections are typified by hemorrhagic fever with renal syndrome (HFRS) mostly caused by isolates of *Hantaan virus* (HTNV) in eastern Asia and hantavirus pulmonary syndrome (HPS) caused by isolates of *Sin Nombre virus* (SNV), Andes virus and related viruses in Americas [6, 37, 38]. The major target organs appear to be different between these two forms of hantavirus infections: kidneys in HFRS and lungs and hearts in HPS. However, same organs are often affected in both diseases and it is considered that one of the fundamental pathological manifestations is vascular leakage [6, 7, 21, 37, 38].

Both HTNV and SNV infect endothelial and monocytic cells *in vitro* and *in vivo*. Neither hantavirus infections of cultured cells causes obvious cytopathic effects, contrary to some other hemorrhagic fever viruses like filoviruses [17, 36, 39, 43, 45]. In filovirus infection, for example, the disruption of endothelial cells *in vivo* directly relates to the massive vascular leakage [11]. An *in vitro* study showed that HTNV infection induced apoptotic endothelial cell death [16]. Nevertheless, histopathological examinations of either hantavirus-infected patients did not show major endothelial cell death [24, 35, 45]. Further, it was reported that SNV infection of endothelial cell monolayers did not alter the permeability or tight junction structures *in vitro* [17, 42]. It is, therefore, possible that both hantavirus infections affect the function of endothelial cells in a limited fashion.

HTNV-infected patients develop cellular and humoral immune responses before or very soon after the onset of clinical symptoms, leading to a hypothesis that the symptoms are partly due to immunopathogenesis [7]. Animal experiments with HTNV supported this hypothesis [18, 30, 34, 44]. Besides the virus-specific immunity, elevated levels of tumor necrosis factor alpha (TNF-alpha) and interleukin-6 (IL-6) in HFRS patients' sera were reported [22]. In an *in vitro* study, the infection of immature dendritic cells with HTNV weakly up-regulated TNF-alpha production [39]. Similarly, the infection of human alveolar macrophages with SNV *in vitro* resulted in a weak induction of TNF-alpha at around 1 ng/ml in the culture supernatant [17]. Endothelial cells carry two known TNF-alpha receptors, TNF-R75 and TNF-R55 [25, 27]. The effects of TNF-alpha on endothelial cells through these TNF-alpha receptors have been widely investigated. TNF-alpha increases vascular permeability [2, 5, 14, 33, 40]. It induces the release of cytokines and chemokines from endothelial cells [27]. It also up-regulates production of inducible enzymes such as cyclooxygenases-2 (Cox-2) and nitric oxide synthases (NOS) [4, 12, 28]. However, the relevance of these specific and non-specific immune responses elicited by hantavirus infections to their pathogenesis is not yet well understood.

Since neither the increase in permeability of endothelial cell monolayers [42] nor TNF-alpha induction in monocytic cells [17, 39] upon the hantavirus infections *in vitro* alone was accountable levels for the clinical manifestations seen in HFRS, we hypothesized that the low level of pro-inflammatory cytokines produced by HTNV-infected monocytic cells might differently affect HTNV-

infected and uninfected endothelial cells, due to possible functional alterations of the HTNV-infected endothelial cells. In order to test this hypothesis, we compared the responses of HTNV-infected and uninfected human umbilical vein endothelial cells (HUVEC) to low concentrations of cytokines.

Materials and methods

Cells and viruses

Pooled primary HUVEC was purchased from Clonetics (San Diego, CA). HUVECs were expanded and maintained in EGM-2 medium supplemented with growth factors and 2% bovine fetal serum (Bullet kit, Clonetics) as recommended by the supplier. The cells were cultured at 37 °C with 5% CO_2 throughout the experiments. HTNV strain 76–118 was provided by Dr. J. Arikawa (Hokkaido University, Japan) and propagated in Vero E6 cells.

Cytokines, antibodies and specific inhibitors

Recombinant human TNF-alpha was purchased from Lifetech (Rockville, MD). The specific activity was $>2 \times 10^7$ units/mg. Recombinant human IL-6 was purchased from Genzyme (Cambridge, MA). Neutralizing polyclonal antibodies specific to TNF-alpha and IL-6, respectively, were purchased from R&D systems (Minneapolis, MN). Neutralization of TNF-alpha prior to stimulation was achieved by mixing 100 ng/ml TNF-alpha and 50 μg/ml antibody and incubation on ice for 1.5 hr. Polyclonal rabbit antiserum to *Seoul virus* (a hantavirus species) strain SR-11 was prepared in our laboratory by inoculation of the live virus to a rabbit [41]. This antiserum was cross-reactive with HTNV. Monoclonal antibody specific to plakoglobin was purchased from Zymed (South San Francisco, CA). Specific inhibitors for NOS and Cox, aminoguanidine and L-NMA, and indomethacine, respectively, were purchased from Sigma (St. Lois, MO). They were used at the concentrations reported effective, respectively [8, 15, 28].

Preparation of HTNV-infected HUVEC

HUVECs were infected with HTNV at the passage level one and further passed twice. At the passage level of three in total, the HTNV-infected cells were frozen as aliquots in liquid nitrogen. Uninfected cells were similarly passed and frozen at the same passage level. The frozen cells were thawed and cultured in tissue culture flasks. These cells were trypsinized, counted and subjected to the experiments. The HTNV-infected and uninfected HUVECs were compared at the same passage levels between four and six. The percentage of HTNV-infected cells at the passage level four was greater than 50%, when determined by an immunofluorescent assay using the antiserum to Seoul virus. The absence of mycoplasma in both HTNV-infected and uninfected HUVECs was confirmed by a PCR-based kit (Mycoplasma Plus PCR Primer Set, Stratagene, La Jolla, CA).

Transmonolayer electrical resistance (TER) of HUVEC monolayers

TER of the HUVEC monolayers was examined by Endome chamber (World Precisions, Saratoga, FL). HUVECs were plated at a density of 1×10^5 cells per well in Transwell-col (0.33 cm^2 growth area, Coaster, Cambridge, MA) with 0.6 and 0.1 ml of the culture medium in the lower and upper chambers, respectively. The growth area was pre-coated with fibronectin according to the method by Bonner and O'Sullivan [3]. On the next day, the culture medium was carefully removed and the cells were re-fed with the same volumes of medium. Two or three days later, designated as time 0, the TER was measured in Endome chamber filled with

0.6 ml of the medium. All the reagents added to the wells were prepared in the medium as 100× concentrations to the final concentrations, and 1 μl was added to 0.1 ml of the medium present in the upper chambers. All the experiments were performed in triplicate and the results were expressed as averages and standard deviations (SD). The measured resistance was converted to net resistance per cm^2 according to the formula:

"Net resistance per cm^2"
= "[Measured resistance (ohm)-21(ohm, resistance without cell monolayer)]/3"

Permeability assay

Permeability of the HUVEC monolayers was examined as described previously [3]. Briefly, 1 g of bovine serum albumin (BSA, Sigma) was stained with 45 mg of trypan blue (Sigma) by mixing in 5 ml of the medium at room temperature (RT) for 2 hr. The binding of trypan blue to BSA was confirmed by precipitating the stained BSA by trichroloacetic acid. After centrifugation, the remaining free trypan blue in the supernatant was less than 0.07% in comparison with the pre-precipitation solution, when determined by the absorbance at 550 nm. The stained BSA was filter sterilized. To measure the leakage through cell monolayers, 10 μl of the stained BSA was added to the upper chamber of each Transwell containing HUVEC monolayer. After 4 hr of incubation, 100 μl of the medium in lower chambers was removed and the absorbance was measured at 550 nm.

Cell viability assay

Cell viability was examined by Cell Counting Kit-8 (CCK-8), which utilizes water-soluble tetrazolium salt (Dojin Chemical, Tokyo, Japan). The HTNV-infected and uninfected HUVECs were plated in 96-well tissue culture plates pre-coated with fibronectin, at a density of 1×10^5 cells per well in 200 μl of the medium. On the next day, the medium was completely replaced and cells were cultured for additional 2 days. Then TNF-alpha was added to the medium at a final concentration of 1 ng/ml. After 72 hr culture, 10 μl of the tetrazolium salt solution supplied in CCK-8 was added to each well and incubated for 1.5 hr. The culture supernatant (100 μl) was transferred to another 96-well plate and the absorbance was measured at 450 nm by a microplate reader with the reference wavelength at 600 nm.

Immunohistochemistry

The HTNV-infected and uninfected HUVECs were cultured on cover slips pre-coated with fibronectin in 48 well tissue culture plates at a density of 3×10^5 cells per well in 400 μl medium. Prior or after the TNF-alpha treatment, the cells were fixed in 4% formaldehyde at RT. The cells were permealized by 2% NP-40 and stained by anti-plakoglobin mouse monoclonal and anti-Seoul virus rabbit polyclonal antibodies. The reacted antibodies were detected by either FITC-labeled anti-mouse IgG (Zymed) or Rhodamine-labeled anti-rabbit IgG (Jackson ImmunoResearch, West Grove, PA), respectively.

Cytokine assays

IL-6, TNF-alpha and IL-1beta were quantitated by Quantikine ELISA kits (R&D Systems). The HTNV-infected and uninfected HUVECs (2.5×10^5 cells) were plated in 1 ml medium in 24 well tissue culture plates pre-coated with fibronectin. The medium was replaced on the

next day and cultured for additional 2 days. Before the addition of 1 ng/ml of TNF-alpha, the first sample was collected (time 0). After the indicated hours of culture, the supernatant (100 μl) was recovered from each well. The supernatants were kept at −80 °C until use.

Statistical analyses

Student's T-tests were performed using Microsoft Excel software.

Results

Effect of TNF-alpha on HTNV-infected endothelial cell monolayers

The transmonolayer electrical resistance (TER) of HUVEC monolayers was not changed by HTNV infection alone (Fig. 1A, time 0). The TER of HTNV-infected and uninfected monolayers was between 10 and 20 ohm/cm^2, which was comparable to the previous reports [2]. TNF-alpha significantly decreased the TER of HTNV-infected and uninfected monolayers at 1 ng/ml (Fig. 1A) and 10 ng/ml, but not at 0.1 ng/ml (data not sown). The HTNV-infected and uninfected monolayers showed similar levels of TER decrease as early as 4 hr after the addition of 1 ng/ml of TNF-alpha (Fig. 1A). The duration of the effect was, however, significantly different between the HTNV-infected and uninfected monolayers. In the uninfected monolayers, the decreased TER started to recover after 24 hr

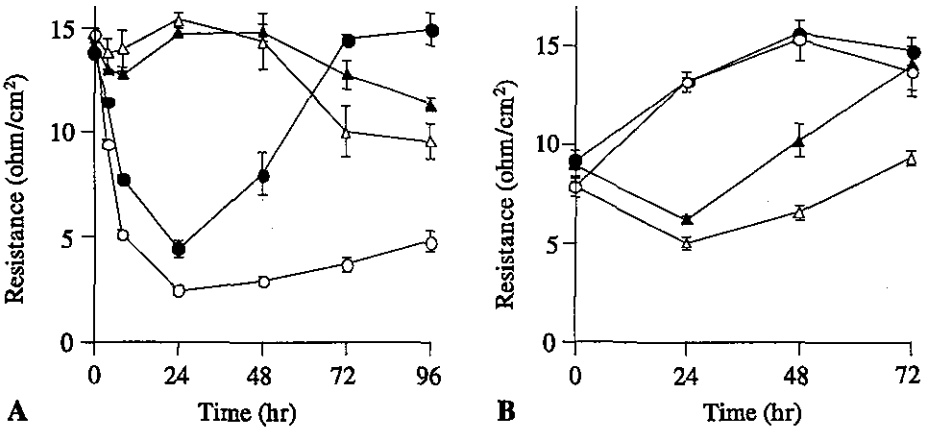

Fig. 1. Effect of TNF-alpha at 1 ng/ml on transmonolayer electrical resistance (TER) of HTNV-infected and uninfected HUVEC. **A**. HTNV-infected (○) and uninfected (●) monolayers were stimulated by TNF-alpha at time 0 and the TER was measured at 4, 8, 24, 48, 72 and 96 hr after stimulation. Unstimulated controls of HTNV-infected (△) or uninfected (▲) HUVEC monolayers were included. **B**. Contribution of TNF-alpha to the decreased TER after TNF-alpha stimulation. TNF-alpha was mixed with neutralizing antibody specific to TNF-alpha. After 1.5 hr incubation on ice, the neutralized (○, infected; ●, uninfected) or mock-neutralized (△, infected; ▲, uninfected) TNF-alpha was added to the HUVEC cultures. The TER was measured at 4, 8, 24, 48 and 72 hr after stimulation. Each point represents the mean value of triplicate. Bars indicate SD

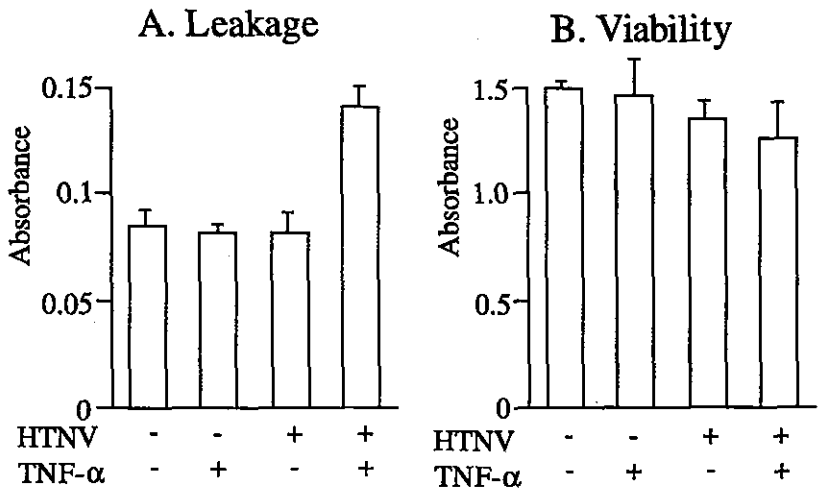

Fig. 2. A. Compatibility of decreased TER with increased permeability. Influx of stained BSA through the HTNV-infected (HTNV+) or uninfected (HTNV−) HUVEC monolayers was quantitated by the absorbance at 48 hr after TNF-alpha stimulation. The TER (average ± SD) at this time point for uninfected unstimulated, uninfected stimulated, infected unstimulated and infected stimulated monolayers were 13.8 ± 0.51, 20.3 ± 0.88, 15.8 ± 0.51 and 8.3 ± 0.33, respectively. **B.** Increased permeability was not due to cell death. Viabilities of HUVEC were examined at 72 hr after TNF-alpha stimulation (1 ng/ml) by the tetrazolim salt color development and shown as the absorbance of each supernatant. Each value represents the mean value of triplicate. Bars indicate SD

and reached the control level within 72 hr. Contrary, the decreased TER did not recover to the untreated level in the HTNV-infected monolayers even at 96 hr. The TER difference between uninfected and HTNV-infected monolayers at 72 hr after stimulation was statistically significant ($p < 0.01$). This decrease of TER was truly induced by TNF-alpha, since the anti-TNF-alpha neutralizing antibody completely abolished the decrease (Fig. 1B). The anti-TNF-alpha antibody itself showed no effect on the TER (data not shown).

To examine if the decreased TER actually reflected the increase in the permeability of monolayers, passive diffusion of BSA through the monolayers was examined (Fig. 2A). At 48 hr, when the HTNV-infected and uninfected monolayers showed significantly different TER ($p < 0.01$), the influx of stained BSA through the infected monolayers was significantly increased ($p < 0.05$) compared to the uninfected ones, indicating that the TER truly reflected the permeability. Further, the increase in permeability was not due to major cell death, since cell viability of these monolayers was not significantly different ($p > 0.05$) between the HTNV-infected and uninfected ones at 72 hr (Fig. 2B).

At any time point of TNF-alpha treatment, the peripheral localization of plakoglobin, which is a sensitive indicator for the matured endothelial cell-to-cell junctions [20], was not disturbed, suggesting that the junction structure was not destroyed by HTNV infection or this TNF-alpha treatment (Fig. 3). These results

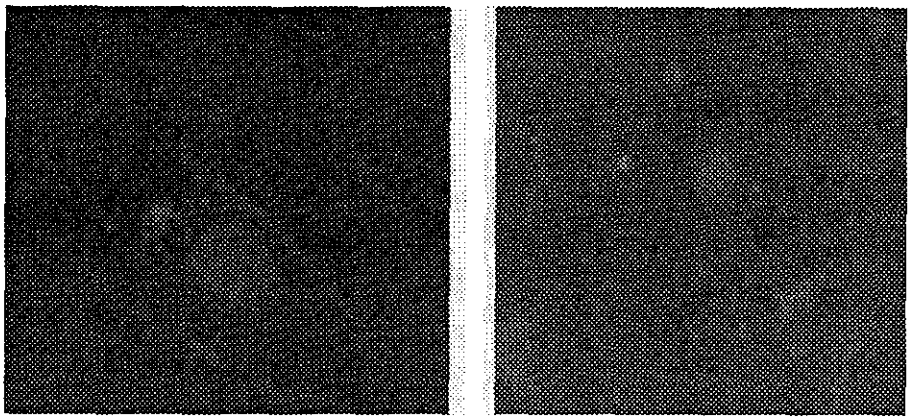

A. Infected B. Uninfected

Fig. 3. Maintenance of cell-to-cell junction structures after TNF-alpha stimulation. HUVEC monolayers were stained by anti-plakoglobin and anti-Seoul virus (cross-reactive with HTNV) antibodies then visualized with FITC (green)- or Rhodamine (red)-labeled secondary antibodies, respectively. **A** HTNV-infected HUVEC at 72 hr after TNF-alpha stimulation. **B** Uninfected non-stimulated control HUVEC at 72 hr

indicate that the HTNV-infected and uninfected HUVEC monolayers show similar levels of initial hyper-permeability without major cell death upon the exposure to TNF-alpha, but the increased permeability remains for a prolonged period in the HTNV-infected monolayers.

Effect of antagonists to NOS and Cox on TNF-alpha-induced hyper permeability

It is known that TNF-alpha induces both nitric oxide (NO) and prostaglandin (PG) through the induction of NOS and Cox-2, respectively. We examined whether NO and PG were involved in the different time courses of the response between HTNV-infected and uninfected monolayers. Aminoguanidine and L-NMA are specific inhibitors for inducible NOS (iNOS) and endothelial NOS (eNOS), respectively. As shown in Fig. 4A and B, neither aminoguanidine (100 μM) nor L-NMA (1 mM) altered the responses of HTNV-infected and uninfected monolayers to 1 ng/ml of TNF-alpha. When 30 μM of indomethacine, a Cox inhibitor was added, TNF-alpha-induced decrease of TER was not affected both in the HTNV-infected and uninfected cell monolayers (Fig. 4C). These results indicate that either NO or PG is not involved in the longer duration of increased permeability in the HTNV-infected monolayers. In fact, neither of them was involved in the TNF-alpha-induced increase in permeability in the HTNV-infected and uninfected monolayers.

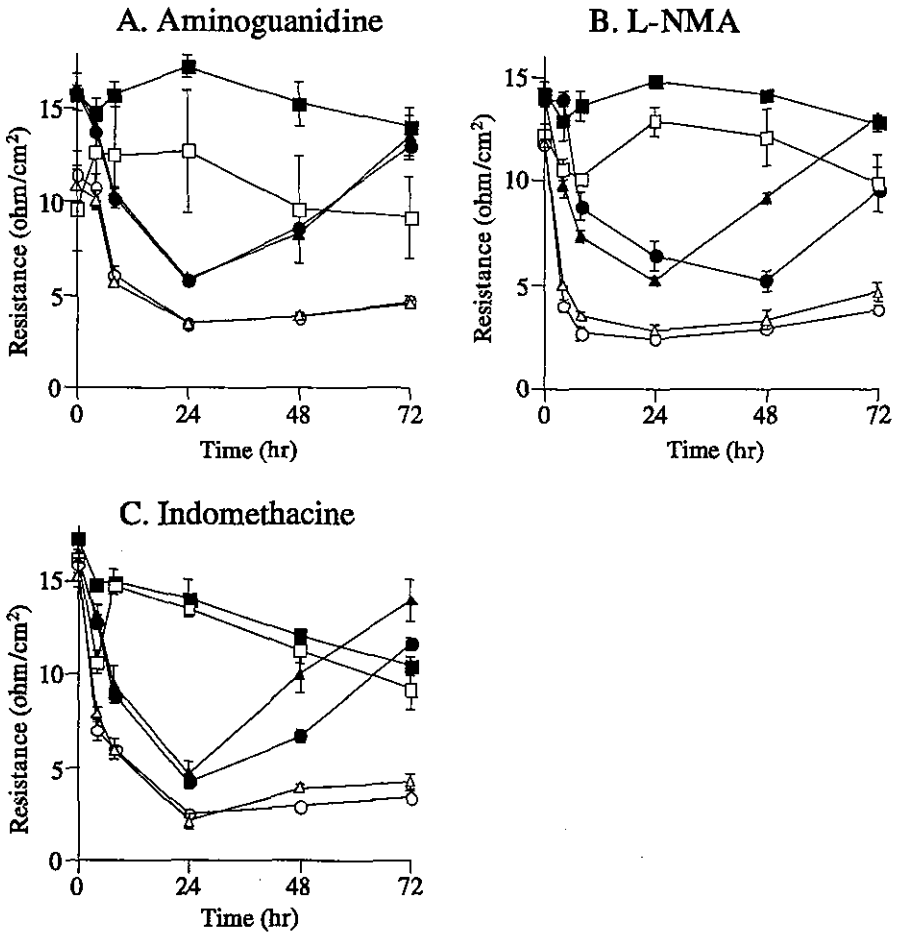

Fig. 4. Absence of the effect of NOS inhibitors and a cyclooxygenase inhibitor on TER. Aminoguanidine (100 μM, iNOS inhibitor, **A**), L-NMA (1 mM, eNOS inhibitor, **B**) or Indomethacin (30 μM, cyclooxygenase inhibitor, **C**) was added along with 1 ng/ml TNF-alpha and the TER was measured at 4, 8, 24, 48 and 72 hr after the stimulation. □, infected control HUVEC; ○, infected TNF-alpha-stimulated HUVEC; △, infected TNF-alpha-stimulated HUVEC with the inhibitor; ■, uninfected control HUVEC; ●, uninfected TNF-alpha-stimulated HUVEC; ▲, uninfected TNF-alpha-stimulated HUVEC with the inhibitor. Each point represents the mean value of triplicate. Bars indicate SD

Induction of pro-inflammatory cytokines by TNF-alpha stimulation

We next asked if the TNF-alpha-induced pro-inflammatory cytokines from endothelial cells might affect the permeability by autocrinal mechanisms. As shown in Fig. 5A, IL-6 was induced at significantly higher levels in the HTNV-infected HUVEC cultures than in the uninfected ones. In the HTNV-infected cells, IL-6 levels increased sharply during the first 24 hr after the stimulation and reached

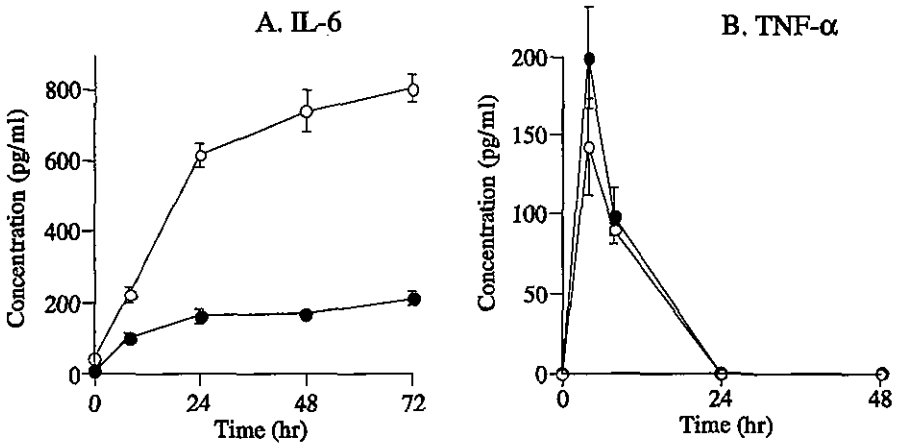

Fig. 5. Induction of high levels of IL-6 and absence of TNF-alpha induction by TNF-alpha. IL-6 (**A**) and TNF-alpha (**B**) concentrations in the supernatants of HTNV-infected (○) and uninfected (●) HUVEC were assayed at indicated hours after the addition of TNF-alpha (1 ng/ml). Time 0 indicates the concentrations before the addition of TNF-alpha. Each point represents the mean value of triplicate. Bars indicate SD

616 pg/ml. The concentration gradually increased further up to 807 pg/ml until 72 hr after the stimulation. On the other hand, in the uninfected cells, the concentration of IL-6 was slowly increased up to 163 pg/ml for the first 24 hr. During the next 48 hr, the concentration slightly increased and reached 210 pg/ml at 72 hr after the stimulation.

The HTNV infection of HUVEC itself did not induce TNF-alpha production (time 0 in Fig. 5B). The TNF-alpha concentration in the supernatants decreased rapidly after the addition of TNF-alpha, probably due to the degradation or absorbance to the cells, and completely disappeared at 24 hr after the addition. It was not detected thereafter until 96 hr (Fig. 5B and data not shown). At 4 hr after the stimulation, the concentration of TNF-alpha was marginally higher in the uninfected cell supernatant; however, the difference completely disappeared at 8 hr. Thus, the TNF-alpha stimulation did not induce significant level of TNF-alpha in either the HTNV-infected or uninfected HUVECs. IL-1beta was not produced above the detectable levels (10 pg/ml) by the TNF-alpha stimulation either in the HTNV-infected or uninfected HUVECs (data not shown).

We then investigated if the increased level of IL-6 was involved in the extension of hyper-permeability in HTNV-infected monolayers by adding the neutralizing antibody to IL-6 at the time of TNF-alpha stimulation. The antibody at concentrations of 50 or 500 ng/ml did not affect the time courses of hyper-permeability in either the HTNV-infected or uninfected monolayers (data not shown). Further, the uninfected monolayers treated with the mixtures of TNF-alpha and IL-6 did not show prolonged hyper-permeability (data not shown). These results suggest that IL-6 is not involved in the prolonged response of the HTNV-infected monolayers to TNF-alpha.

Discussion

We demonstrated that HTNV infection of HUVEC extended the duration of increased permeability of monolayers induced by low levels of TNF-alpha, while the magnitude of initial increase in permeability was comparable to the uninfected cells. In fact, this phenomenon was observed when 1 ng/ml of TNF-alpha was added to the culture medium, which is 10 times higher concentration than that detected in HFRS patients' sera [22]. This concentration is, at the same time, comparable to the reported concentration secreted by SNV-infected macrophages *in vitro* [17]. This is the first report demonstrating that the infection of hantavirus to endothelial cell monolayers modifies their barrier function. We speculate that the prolonged hyper-permeability of HTNV-infected endothelium induced by the TNF-alpha secreted from the infected monocytic cells may result in a gradual accumulation of hyper-permeable vascular endothelium (Fig. 6). In this hypothetical model, we assume the number of infected monocytic cells and the overall

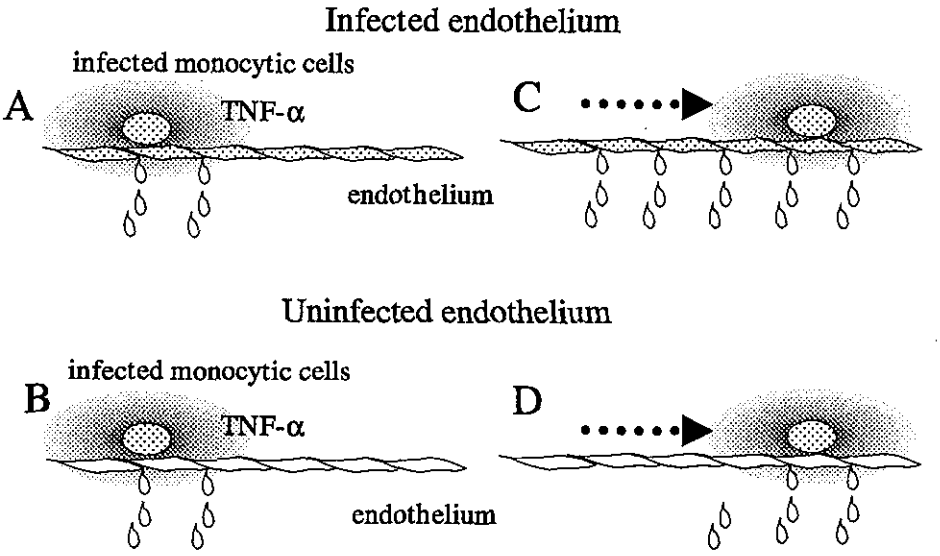

Fig. 6. A hypothetical scheme how the combination of the prolonged hyper-permeability of infected endothelium and the low-level TNF-alpha secretion from infected monocytic cells may contribute to a serious plasma leakage. In both infected and uninfected endothelium, the low-level TNF-alpha from the infected monocytic cells induces hyper-permeability only to the close proximity (**A** and **B**). When the infected monocytic cells move, plasma discharge continues from the infected endothelium which is no longer close proximity to the infected monocytic cells, as well as the leakage from the endothelium now becomes close proximity to them (**C**). Contrary, in the uninfected endothelium, only the endothelium newly becomes close proximity to the infected monocytic cells begins to leak, while the previously hyper-permeable endothelium recovers when the concentration of TNF-alpha is not high enough any more (**D**)

amount of secreted TNF-alpha from these cells are not great enough to induce systemic catastrophic change. On the other hand, the secretion of TNF-alpha from individual infected monocytic cell is high enough to induce prolonged hyper-permeability in the proximal infected endothelium. This might contribute to a local catastrophic plasma leakage after a certain period of time in specific organs where the infected endothelial cells and monocytic cells are close proximity. It should be noted that although HFRS is an acute disease, it takes order of weeks after infection before the critical condition appears [19]. A recent report showed that HTNV infection also induced dendritic cells to produce a low level of TNF-alpha [39]. Thus, the HTNV-infected monocytic cells can be a source of TNF-alpha *in vivo*, though TNF-alpha was supplied exogenously in our *in vitro* experiments. Of further interest, increased numbers of TNF-alpha producing cells in HPS patients' lungs were described and the involvement of local cytokine production in the HPS pathogenesis was suggested [32]. Furthermore, in dengue virus infection, which also causes hemorrhagic fever without serious damage on vascular endothelium, it was reported that TNF-alpha from the dengue virus-infected peripheral monocytes modulated endothelial cell protein expressions [1]. The mechanisms behind the hyper-permeability without disruption of the tight junction are not clear. One report suggested that the rearrangement of cytoskeleton by TNF-alpha changed the tension within the individual cells and resulted in hyper-permeability in endothelial monolayers without gap formation [2].

In HFRS and HPS patients' plasma, increased levels of NO were reported [9, 24]. In the former, the increased NO levels correlated to the TNF-alpha levels. However, our results suggested that NO was not involved in the prolonged hyper-permeability. The irrelevance of NO to the formation of pulmonary edema and alveolar flooding in a mice model system with lymphocytic choriomeningitis virus, which might mimic HPS, was recently reported [9]. The involvement of PG in the prolonged hyper-permeability was also not likely, while Cox-2 was one of the up-regulated genes by the HTNV infection in endothelial cells detected by the DNA array experiments [13].

The low level of TNF-alpha induced IL-6 above 700 pg/ml in the HTNV-infected HUVECs. This phenomenon might partly contribute to the elevated levels of IL-6 in HTNV-infected patients. It is noteworthy that a previous report showed no difference in IL-6 levels between the HTNV-infected and uninfected endothelial cells *in vitro*, as the pre-stimulation levels in our experiments [36]. The involvement of induced IL-6 in the pathogenesis of HTNV infection is not clear, though our data indicates that it is not involved in the prolonged hyper-permeability. In one report, IL-6 alone could induce hyper-permeability at higher concentrations above 20 ng/ml using normal bovine endothelial cell monolayers derived from carotid aorta [29]. In our study, HUVEC monolayers did not respond to IL-6 alone at concentrations up to 100 ng/ml (data not shown). Since endothelial cells derived from different organs or species may show different property [2, 26], it is not known whether this is due to the difference of source organs of the endothelial cells or to the species difference.